Supporting Information

Boque-Sastre et al. 10.1073/pnas.1421197112

SI Materials and Methods

Cell Culture. HCT116, Caco-2, and SW480 human colon adenocarcinoma cell lines were cultured in DMEM (PAA Laboratories) containing stable glutamine, and supplemented with 10% (vol/vol) [20% (vol/vol) for Caco-2] heat-inactivated FBS (Invitrogen) and 1% penicillin–streptomycin (PAA Laboratories). MCF7 breast adenocarcinoma was cultured under the same conditions, but the medium was supplemented with 0.01 mg/mL human recombinant insulin. Nonmalignant MCF10A breast cells were grown in DMEM/Ham's F-12 medium (PAA Laboratories) supplemented with 20 ng/mL EGF (E9644; Sigma), 500 ng/mL hydrocortisone (H0888; Sigma), 10 mg/mL insulin (I0516; Sigma) and 100 ng/mL cholera toxin. All cells were grown at 37 °C in a humidified atmosphere of 5% (vol/vol) CO_2 and 95% (vol/vol) air.

Human Sample Methylation Analysis on Illumina's 450K Bead-Chip Array. DNA preparation, bisulfite conversion, and the analysis of methylation levels were done as described (1). An unpaired-samples Student's *t* test was performed to check for differentially methylated probes between normal and tumor samples. Comparisons with a difference in average beta value greater than 25% and an adjusted value of *P* (FDR) < 0.01 were considered to be statistically significant. DMR was defined as the region containing CpG sites with a significant corrected *P* value (FDR < 0.01) from a 2×2 χ^2 contingency test of the association of methylated and unmethylated cytosines with normal and tumor samples.

PolyA$^+$/PolyA$^-$ RNA Selection and Nuclear/Cytoplasmic Fractionation. PolyA$^+$ and polyA$^-$ RNAs were separated by using the Dynabeads mRNA Purification kit (61006; Life Technologies), using three rounds of selection. RNA enrichment in each fraction was then analyzed by RT-qPCR, using *GAPDH* or *U6* RNAs as controls, and normalizing relative to the percentage of RNA from each fraction used in the reverse transcription reaction. Subcellular fractionation was performed with a PARIS kit (Life Technologies; AM1921). Equal amounts of RNA from each fraction were subject to RT-qPCR, and the results were normalized taking into account the total amount of RNA recovered from each fraction. *PPiA* and *U6* RNAs were used as controls for fraction purity.

RNA-FISH and Actinomycin D Treatment. Two pools of 48 probes tiling either the first intron of *VIM-AS1* RNA (starting just downstream of the C skew region to avoid interference with the R-loop region) or the first intron of *VIM* RNA were designed following Stellaris RNA FISH Probe designer (Biosearch Technologies). *VIM-AS1* probes were coupled to TAMRA and *VIM* probes to FAM reporter dyes. Cell fixation, permeabilization, and probe hybridization were performed by following Stellaris FISH Protocols for adherent cells, with Vectashield Hardset (H1400; Vector Laboratories) as mounting medium. For actinomycin D experiments, synchronized cells were allowed to progress for 6 h into the G_2 phase and treated with either DMSO or 5 μg/mL actinomycin D (Sigma) for 30 min, before cell fixation and RNA-FISH analysis, RAP assays or RT-qPCR experiments.

DNA Methylation Analysis and in Vivo R-Loop Detection. DNA methylation was determined by PCR analysis after bisulfite modification of genomic DNA. Region 1 was amplified with primers bsVIM_R1for and bsVIM_R1rev and region 2 with primers bsVIM_R2for and bsVIM-R2rev (Table S1). In vivo R loop was detected in SW480 cells in essentially the same way but with native overnight treatment with sodium bisulfite at 37 °C. The PCR was performed with a forward, native oligonucleotide (N in Fig. 5*C*) outside the C skew-containing region and a reverse, converted oligonucleotide (C in Fig. 5*C*), which takes into account the C-to-U changes (C-to-T after PCR) that occur only on the minus DNA strand following native bisulfite conversion. Following DNA purification, 32 cycles of PCR were carried out with the native forward primer (RLoop_st+_1_F1) and the converted reverse primer (RLoop_st+_1_R1) (Table S1).

Real-Time RT-qPCR. Total RNA from cell lines was extracted by using the TRIzol reagent (Invitrogen) and DNase treated with RQ1 DNase (Promega). For mRNA expression analysis, purified total RNA was reverse-transcribed by using the SuperScript III First-Strand Synthesis System for RT-PCR (Invitrogen). Real-time PCRs were performed in triplicate in an Applied Biosystems 7900HT Fast Real-Time PCR system, using 100 ng of cDNA, 6 μL of SYBR Green PCR Master Mix (Applied Biosystems) and 416 nM primers (listed in Table S1) in a final volume of 12 μL for 384-well plates. All data were normalized with respect to two housekeeping genes (L13 and PBGD), with no significant GC skew at their promoters as endogenous control. Relative RNA levels were calculated by using the comparative C_t method ($\Delta\Delta C_t$), considering the PCR efficiency. The order of magnitude of change is equal to $10^{\Delta\Delta Ct/m}$, where m is the average slope of the calibration curves for the gene of interest and the endogenous control.

Western Blot. Cell pellets were resuspended in lysis buffer (10% glycerol, 2% SDS wt/vol, 63 mM Tris·HCl pH 6.8, 0.01% bromophenol blue, 2% 2-mercaptoethanol), sonicated, and boiled for 5 min. Equal amounts of protein extracts were loaded onto Tris-Glycine-SDS gels and transferred to a nitrocellulose membrane (Whatman; GE Healthcare). Primary antibodies were diluted in 5% skimmed milk in TBS and incubated overnight at 4 °C. Final antibody concentrations were 1:5,000 for vimentin (CBL202; Millipore), 1:1,000 for RNaseH1 (H00246243-B01; Abnova), and 1:20,000 for β-actin-HRP (Sigma). After primary antibody incubations, membranes were washed three times (10 min each) with TBS containing 0.05% Tween-20 at RT on a bench-top shaker. Secondary antibodies conjugated to horseradish peroxidase were diluted to a concentration of 1:10,000 in 5% skimmed milk with TBS, containing 0.05% Tween-20. Membranes were incubated with secondary antibody solutions for 1 h at room temperature (RT) in the dark in a bench-top shaker, washed three times (10 min each) with TBS containing 0.05% Tween-20 at RT, and then briefly rinsed in TBS before detection.

Cell Synchronization. MCF10A cells were synchronized by double thymidine block. Cells were treated with 2 mM thymidine for 14 h in medium supplemented with 10% FCS. After washing twice with PBS, cells were cultured in fresh medium/10% FCS for 10 h and treated again for 14 h with medium/10% FCS containing 2 mM thymidine. After washing cells with PBS, the block was released by the incubation of cells in fresh medium/10% FCS (time 0) and the cells were harvested at the indicated times. Cell-cycle progression was detected by flow cytometric analysis.

RAP. The RAP protocol was performed as described by Engreitz et al. (2). Briefly, the 5′ and 3′ ends of the R-loop–forming region on *VIM-AS1* intron were tiled with 10 124-nt antisense RNA probes that had been biotinylated by in vitro transcription. The central region of the R loop was devoid of probes to prevent interference in the RT-qPCR and the qPCR signal. MCF10A cells

were synchronized as described above and cross-linked first with 2 mM DSG for 45 min at room temperature and then with 3% formaldehyde for 10 min at 37 °C. For each purification, 100 ng of biotinylated probes were added to the precleared lysates and the mixture was incubated at 45 °C. The probes were then captured by streptavidin beads, and the elutions for the associated RNA and DNA were performed. As a control, the same experiment was carried out in parallel with probes tiling the unrelated *LINC00085* nuclear RNA or with streptavidin beads without any probe. Recovered RNA and DNA samples were analyzed by RT-qPCR together with 1/10 dilution of the input material. Primer sequences for probe construction are available upon request.

Immunofluorescence. Cells were cultured directly on coverslips and fixed with 4% paraformaldehyde in water for 20 min at RT. Cells were permeabilized with 0.1% Triton X-100 in PBS for 5 min and blocked with 1% BSA for 1 h. Cells were then incubated with vimentin primary antibody (1:200, CBL202; Millipore) for 1 h at RT. Finally, 1:1,000 dilution of fluorescent-labeled secondary antibody from Invitrogen (anti-mouse IgG; A21235) was used. The coverslips were mounted on glass slides by using Mowiol with DAPI. Multicolor immunofluorescence imaging was then performed under a Leica SP5 laser scanning confocal spectral microscope (Leica Microsystems) equipped with Argon, DPSS561, HeNe633, and 405 Diode, and using a 63× oil immersion objective lens (N.A. 1.32). Data were analyzed by using the Fiji program.

DRIP. Genomic DNA was extracted from SW480 cells by SDS/proteinase K treatment and phenol-chloroform extraction and ethanol precipitation. DNA was then digested with HindIII, EcoRI, XbaI, and BamHI restriction enzymes. Samples were then either mock-treated or digested with RNaseH for a further 2 h. After phenol/chloroform extraction and precipitation, samples were resuspended in IP buffer (0.05% Triton X-100 in PBS) and immunoprecipitated with the anti-DNA-RNA hybrid (S9.6) antibody. Retrieved fragments were analyzed by qPCR and compared with appropriate dilution of input DNA. An amplicon from *GAPDH* promoter (lacking target sites for the restriction enzymes above) was used as a negative control.

Extraction of Nuclei and the Micrococcal Nuclease Accessibility Assay. Growing cells were trypsinized and washed twice with cold PBS. Cells were then resuspended in 1 mL of ice-cold RSB (Tris·HCl 10 mM pH 7.5, NaCl 10 mM, $MgCl_2$ 3 mM, protease inhibitors) adding Nonidet P-40 to a concentration of 1% and kept on ice for 10 min. After incubation, cells were centrifuged for 5 min at 800 × *g* at 4 °C. The supernatant was discarded, and nuclei were resuspended in RSB plus Nonidet P-40. Samples were centrifuged for 5 min at 800 × *g* at 4 °C. Nuclei were washed with medium salt buffer without Nonidet P-40 and centrifuged for 5 min at 2,300 × *g* at 4 °C. The supernatant was discarded and the nuclei were resuspended in 1× micrococcal nuclease buffer to give 10^6 nuclei per 800 μL. Nuclei from each cell condition were digested in 15 U of micrococcal nuclease S7 restriction enzyme (Roche Applied Science) in a series of increasing incubations at 37 °C: 0, 2, 5, and 10 min. Reactions were stopped by adding 200 μL of stop solution (20 mM Tris·HCl pH 7.5, 0.6 M NaCl, 1% SDS, 10 mM EDTA, and 400 μg/mL proteinase K) and incubating at 37 °C for 2 h. DNA was purified by phenol/chloroform extraction and ethanol precipitation. Amplicons were amplified and quantified by real-time PCR in an Applied Biosystems 7900HT Fast Real-Time PCR System. Results were normalized with respect to a Sat2 region, which was expected to be extremely compact and, thus, less accessible to micrococcal nuclease. Undigested samples were analyzed relative to 10 min digested samples, because these conditions revealed the maximum differences. Data were then normalized to consider control samples equal to 1.

ChIP. In brief, 5 × 10^6 lentivirus-transfected SW480 cells were seeded on 100-mm dishes. After reattachment, cells were serum-deprived overnight in DMEM supplemented with 0.5% BSA. The following day, cells were stimulated for 30 min with 30 ng/mL TNF-α, washed in PBS and cross-linked twice, first with 2 mM Di (*N*-succinimidyl) glutarate (DSG; Sigma) for 45 min, and then with 1% formaldehyde for 15 min. Cells were lysed in buffer L1 [50 mM Tris·HCl, pH 8.0, 2 mM EDTA, 0.1% Nonidet P-40 (IGEPAL CA-630, Sigma-Aldrich), 10% glycerol, 1 mM DTT, protease inhibitors] for 15 min on ice, and the nuclei pelleted and resuspended in 500 μL of SDS lysis buffer (50 mM Tris·HCl, pH 8.0, 10 mM EDTA, 1% SDS). Chromatin was sonicated in a Bioruptor (Diagenode) to obtain chromatin fragments of about 150–400 bp. Eighteen A_{260} units of chromatin were used as the input for each immunoprecipitation. Chromatin extracts were precleared overnight with 20 μL of Dynabeads M-280 Sheep Anti-Rabbit IgG (Invitrogen). 4 μg of NfkappaB (p65) rabbit polyclonal antibody (Santa Cruz Biotechnology; sc-109), 1 μg of rabbit polyclonal antibody against H3 (ab1791; Abcam), or 2 μg of normal rabbit IgG control antibody (12–370; Millipore) were coupled overnight to 20 μL of Dynabeads. Precleared extracts were incubated with the Ab–beads complexes for 4 h at 4 °C. After washing, the recovered material was reverse cross-linked with proteinase K, phenol/chloroform extraction, and ethanol precipitation. Immunoprecipitated DNA and 1:50 diluted input sample were analyzed in triplicate by real-time qPCR analyses by using SYBR-Green Master Mix in an ABI 7900 FAST sequence detection system. The primers used are shown in Table S1.

Plasmid Construction and Transfections. Human RNaseH1 lacking the *N*-t mitochondrial localization signal (MLS) was cloned with oligos RNaseHdelMLSEcoRIfor and RNaseHBamHIrev into the EcoRI and BamHI sites of lentiviral expression vector pLVX-IRES-ZsGreen1 (Clontech). shRNA2 and shRNA3 target the 5′ GGTGTACTAGTGAAGTGAT 3′ and 5′ TCCAAATGTGCTACTCAGA 3′ sequences, respectively, of *VIM-AS1* mRNA (both located on the last exon), and were expressed by cloning oligos shVIMAS2for and shVIMAS2rev (for sh2) and shVIMAS3for and shVIMAS3rev (for sh3) into the BamHI and EcoRI sites of vector pLVX-shRNA2 (Clontech). Table S1 contains the full list of oligos used for cloning.

For lentivirus-mediated construct overexpression, HEK293T cells were transfected with pLVX-IRES-ZsGreen1-RNaseH1 construct or pLVX-shRNA2-constructs plus packaging plasmids with jetPRIME (Polyplus-transfection) according to the manufacturer's recommendations. Forty-eight hours after transfection, the supernatant containing viral particles was used to infect target cell lines. ZsGreen1 was used in both cases as a marker to visualize transductants by fluorescence microscopy. In the case of SW480 cells, RNaseH1-transfected cells were enriched by fluorescence-activated cell sorting (FACS) before extract preparation and Western blot analysis.

Transfection with antisense oligonucleotides (LNA GapmeRs, 300600; Exiqon) was carried out as follows: SW480 cells were seeded at 1 × 10^6 cells per well in six-well plates. Transfection mixes were prepared by using HiPerfect (Qiagen) and LNA GapmeRs to a final concentration of 65 nM. Cells were retransfected 48 h later and collected 72 h after the second round of LNA treatment. A control LNA GapmeR (300610; Exiqon) was used as mock transfection.

1. Sandoval J, et al. (2011) Validation of a DNA methylation microarray for 450,000 CpG sites in the human genome. *Epigenetics* 6(6):692–702.

2. Engreitz JM, et al. (2013) The Xist lncRNA exploits three-dimensional genome architecture to spread across the X chromosome. *Science* 341(6147):1237973.

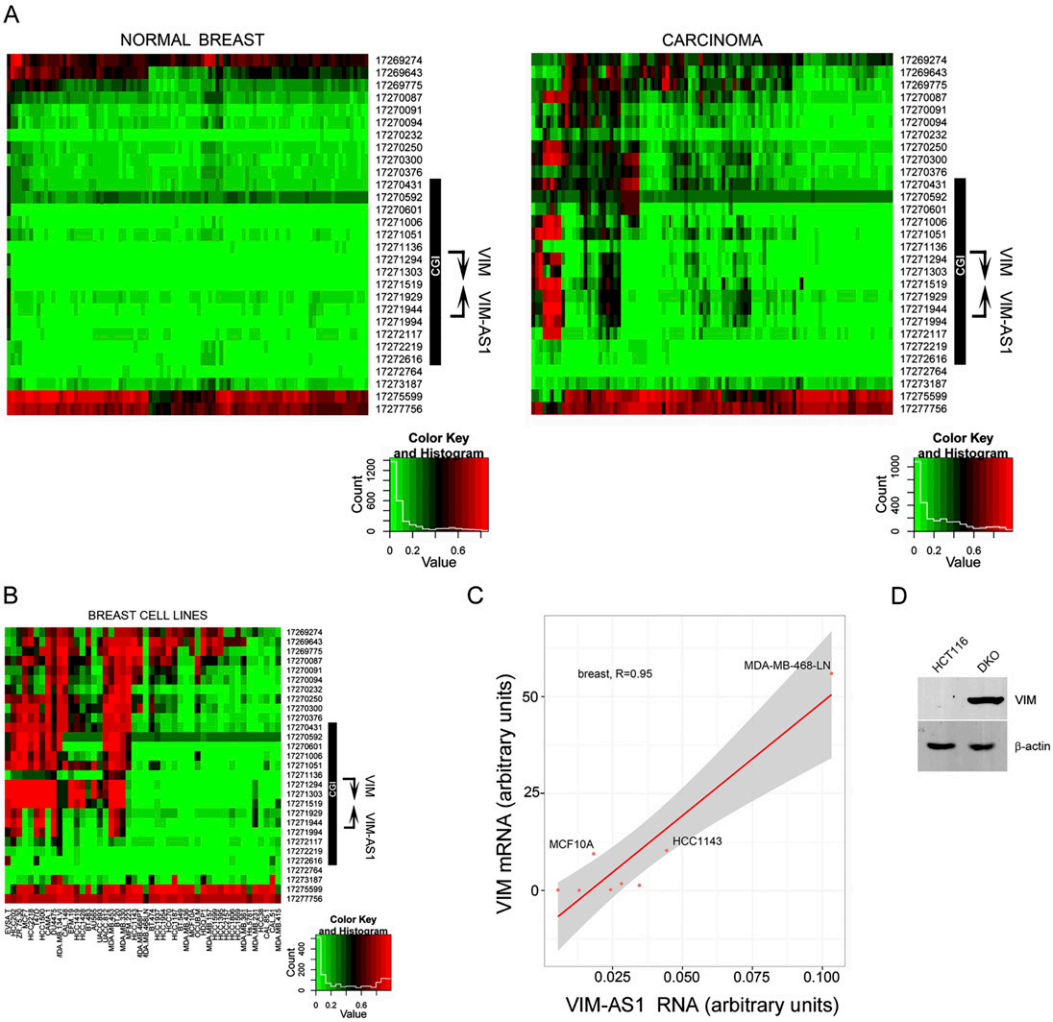

Fig. S1. Sense/antisense transcripts at the vimentin locus are positively correlated and reduced in hypermethylated contexts: related to Fig. 2. (*A*) Heatmap representation of a DNA methylation microarray analysis of 97 human normal breast (*Left*) and 97 tumor (*Right*) samples indicates that hypermethylation of *VIM* promoter CGI is a hallmark of cancer. Individual samples are represented along the horizontal axis. CpG sites surrounding *VIM* and *VIM-AS1* transcription start sites are displayed vertically, with the exact CpG coordinate on chromosome 10 indicated. The CGI is represented as a thick line to the right of each plot. (*B*) Heatmap representation of a DNA methylation microarray analysis of 48 human breast adenocarcinoma cell lines (indicated along the *x* axis). (*C*) Positive Pearson's correlation coefficients between *VIM* (*y* axis) and *VIM-AS1* (*x* axis) expression values for eight breast cell lines (HCC1143, MCF10A, MDA-MB-468 LN, MDA-MB-468 PT, MCF7, T47D, MDA-MB-134 VI, BT-474) indicate coordinated expression. The linear trend is displayed. MDA-MB-468-LN, MCF10A, and HCC1143 cell lines, with a hypomethylated CGI, have the highest levels of expression for both transcripts and are highlighted in the plot. (*D*) Promoter CGI hypermethylation is inversely correlated with vimentin protein levels. Western blot analysis of HCT116 colon cell line (hypermethylated at *VIM* promoter CGI) and its derivative DKO (hypomorph of DNMT1 and DNMT3b and hypomethylated at *VIM* promoter CGI).

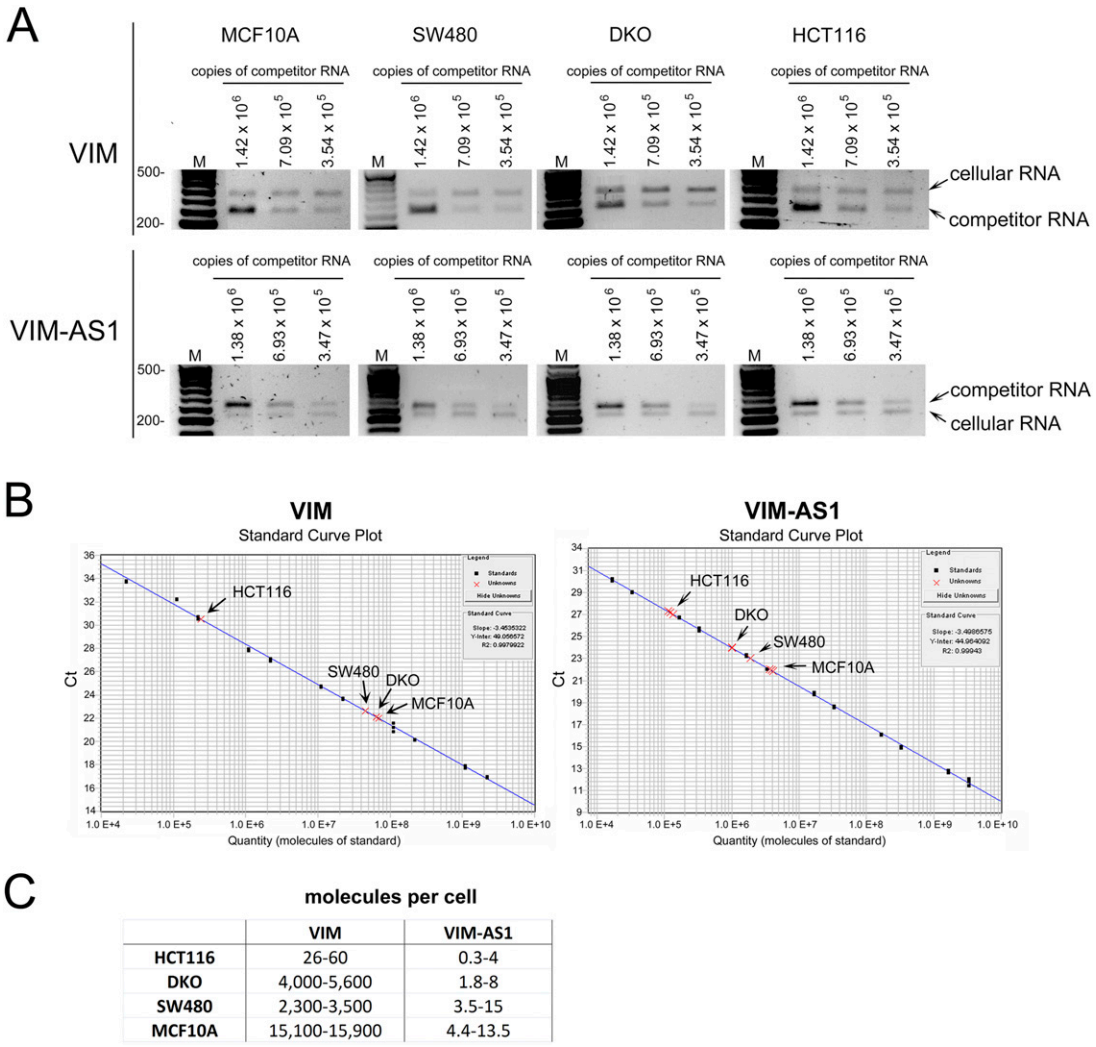

	VIM	VIM-AS1
HCT116	26-60	0.3-4
DKO	4,000-5,600	1.8-8
SW480	2,300-3,500	3.5-15
MCF10A	15,100-15,900	4.4-13.5

Fig. S2. Absolute quantitation of *VIM* AND *VIM-AS1* transcripts. (*A*) Semiquantitative RT-PCR of total RNA from the cell lines indicated in comparison with in vitro transcribed competitor RNA. The competitor RNA is identical to the endogenous amplicon but for the inclusion of a 40-nt spacer sequence (in the case of *VIM-AS1*) or a deletion of 75 nt (in the case of *VIM*), resulting in PCR bands of slightly different size that can be resolved in an agarose gel. The amount of competitor RNA included in the PCR is indicated. The amount of total RNA used of each cell line was as follows: for MCF10A, SW480, and DKO, 0.16 ng in *VIM* PCR and 4 ng in *VIM-AS1* PCR. For HCT116, 12 ng in *VIM* PCR and 40 ng in *VIM-AS1* PCR. (*B*) RT-qPCR using in vitro transcribed templates as standard for comparison. Increasing amounts (indicated in graphs) of *VIM* or *VIM-AS1* standards and 40 ng of total cellular RNA were retrotranscribed and amplified in parallel by qPCR. Absolute abundance for each transcript was estimated by Ct comparison with the standard curve. Ct values corresponding to each cell line tested are indicated by the red crosses. (*C*) Absolute estimations of number of *VIM* and *VIM-AS1* molecules per cell, derived from both semiquantitative and quantitative RT-PCR.

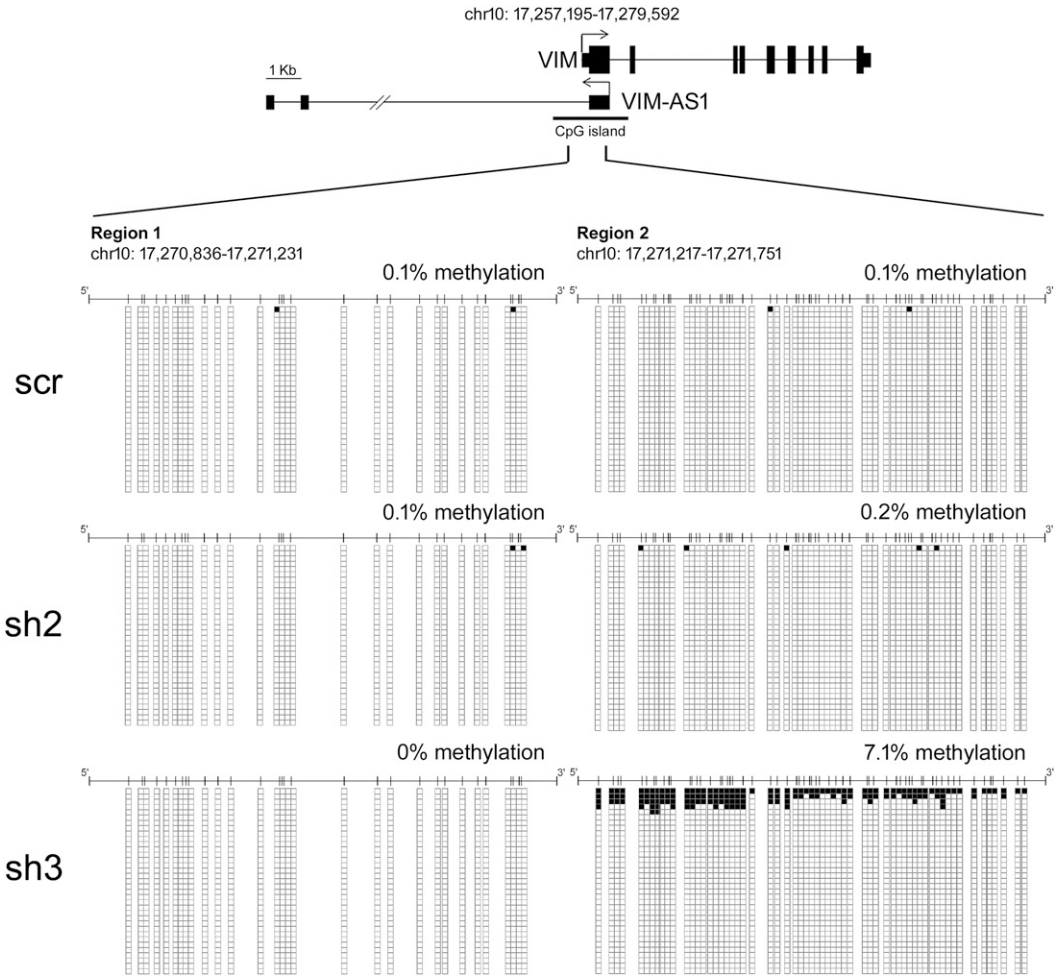

Fig. S3. DNA sequencing following bisulfite treatment of regions 1 and 2 within *VIM* promoter CGI upon shRNA-mediated knockdown.

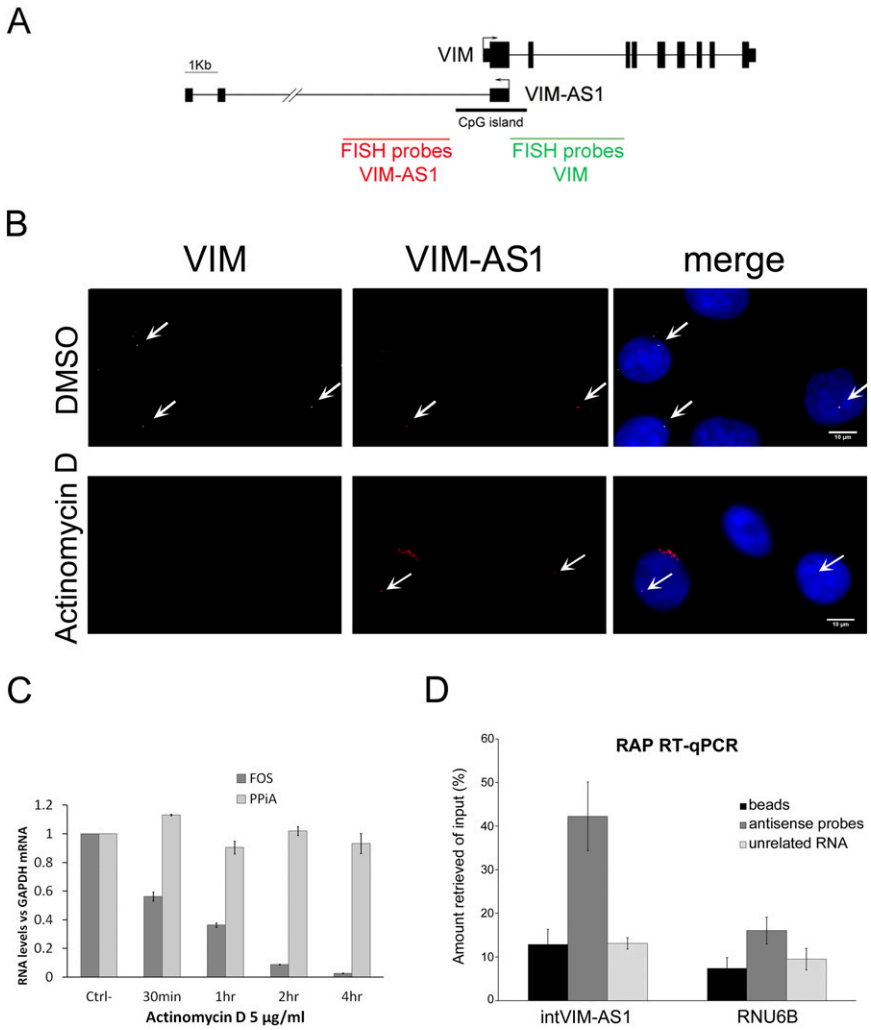

Fig. S4. VIM-AS1 intron 1 locates to the transcription site even upon Act. D treatment and can be recovered in RAP experiments: related to Fig. 4. (*A* and *B*) RNA FISH with probes targeting *VIM* intron 1 (in green) or *VIM-AS1* intron 1 (in red) in control (DMSO-treated) or actinomycin D-treated MCF10A cells. Cell nuclei were stained with DAPI. (*C* and *D*) Reverse transcription-qPCR of the RNA captured in cross-linked MCF10A cells treated as in *B* by using streptavidin beads alone (beads), with antisense probes to VIM-AS1 intron 1 (antisense probes) or against the LINC00085 RNA (unrelated RNA). Enrichments represent means from two replicate experiments and are relative to the input amount used per pulldown. RNU6B is used as negative control to assess binding specificity.

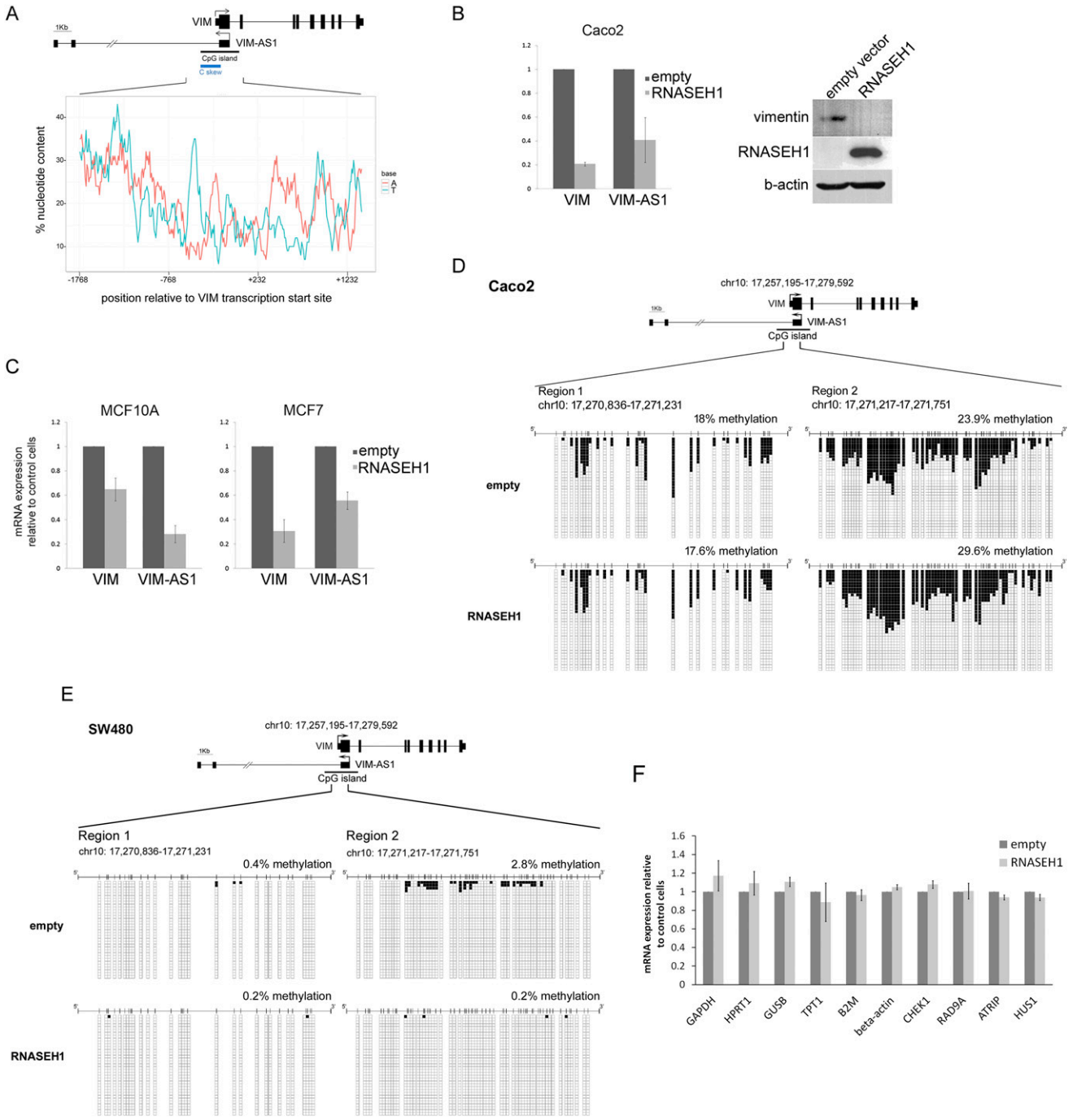

Fig. S5. Overexpression of RNASEH1 reduces *VIM* expression and is accompanied by a slight change in DNA methylation: related to Fig. 5. (*A*) Percentage of A and T nucleotides in the *VIM* promoter. The sequence shown corresponds to the plus strand, and for each position, the percentage abundance of each nucleotide within the surrounding 100 nt is counted, with a sliding window of 1 nt. For clarity, only A (red line) and T (blue line) nucleotides are displayed. The C skew-containing region shown in Fig. 5*A* is indicated by the discontinuous blue line. (*B*) Overexpression of RNASEH1 in Caco2 cells reduces both *VIM* and *VIM-AS1* mRNA expression, as measured by RT-qPCR (*Left*) and vimentin protein levels, as revealed by Western blot (*Right*). Error bars, SDs from three independent experiments. (*C*) Overexpression of RNASEH1 in the nonmalignant breast cell line MCF10A and the breast adenocarcinoma MCF7 reduce *VIM* and *VIM-AS1* RNA expression, as measured by RT-qPCR experiments. Error bars, SDs from three independent experiments. (*D* and *E*) DNA sequencing following bisulfite treatment of regions 1 and 2 within *VIM* promoter CGI reveals a moderate change in methylation upon RNASEH1 overexpression in Caco2 cells but not in SW480 cells. Region 2 overlaps with region 1 so that every CpG dinucleotide is interrogated between coordinates chr10:17,270,836 and 17,271,751 (hg19). Vertical lines represent CpG positions in the whole sequence. Individual clones sequenced are represented horizontally, with empty squares corresponding to unmethylated CpGs and filled squares corresponding to methylated positions. Average methylation levels for each group are indicated. (*F*) RT-qPCR analysis of the mRNA expression levels of the indicated genes in control or RNASEH1-overexpressing SW480 cells.

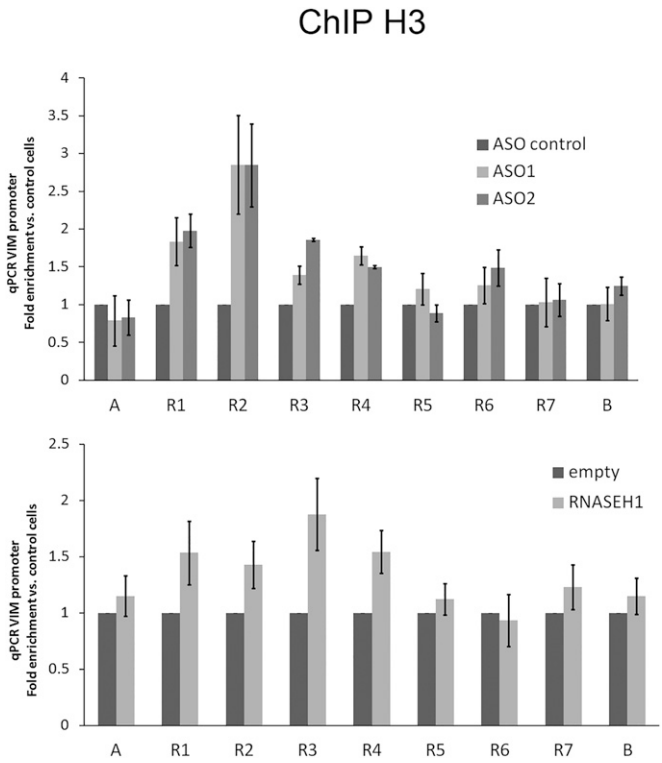

Fig. S6. *VIM-AS1* knockdown or R loop disruption results in an increase in histone H3 density: related to Fig. 6. (*Upper*) ChIP experiments with histone H3 antibody in control (ASO control) or ASOs against *VIM-AS1*-overexpressing SW480 cells. The pulled-down DNA was measured by qPCR, and the values shown are relative to those of the control sample. Regions analyzed are the same as in Fig. 6. (*Lower*) The same experiment but comparing control or RNASEH1-overexpressing cells. Error bars, SDs from three independent experiments.

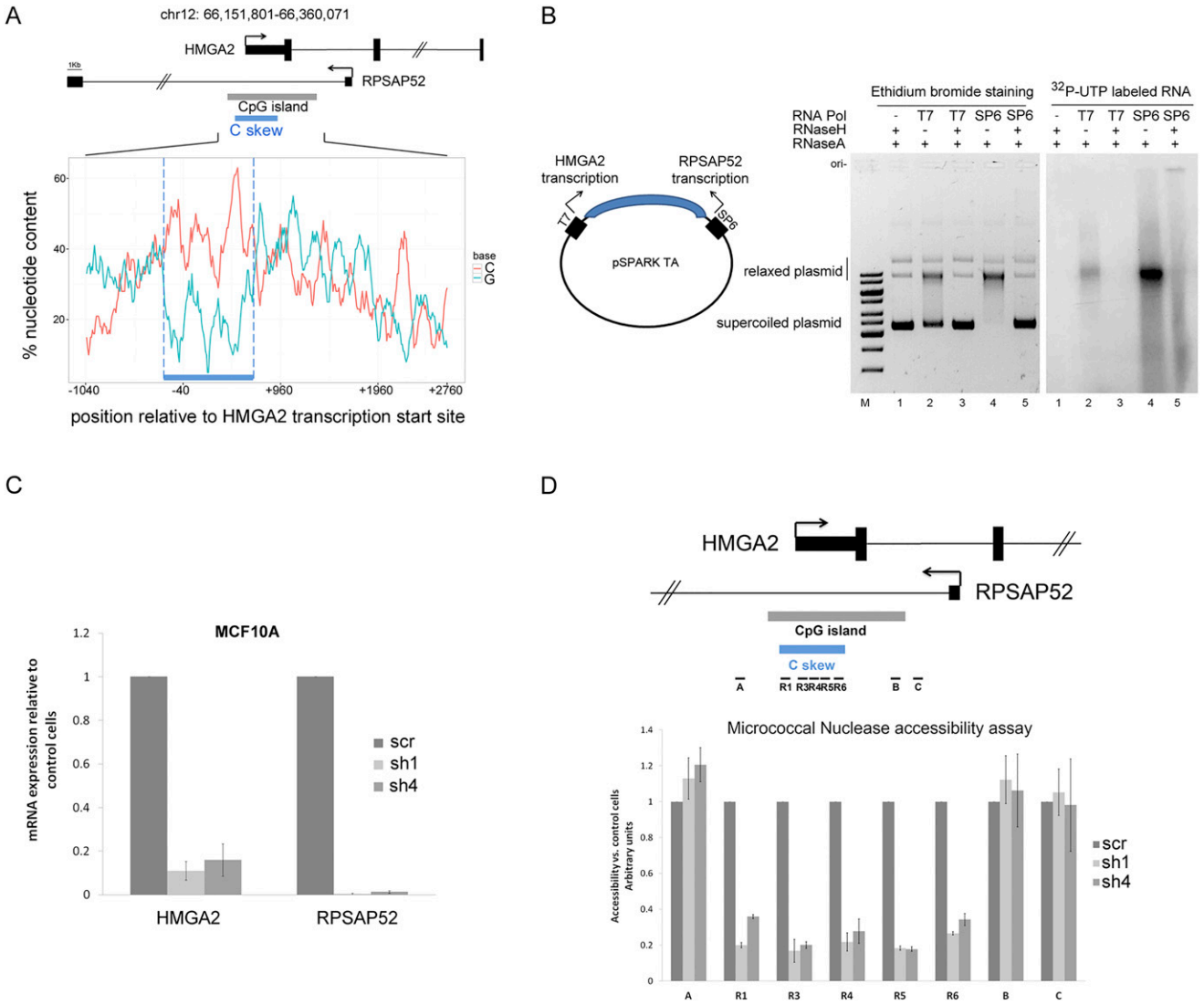

Fig. S7. Antisense-mediated R-loop formation at the *HMGA2* locus promotes open chromatin conformation and sense transcription. (*A*) Percentage of C and G nucleotides in the *HMGA2* promoter reveals the presence of a 1-kb-long C skew. The upper diagram shows the intronic/exonic organization of HMGA2 and its antisense transcript, the pseudogene *RPSAP52*. In the lower plot, the sequence represented corresponds to the plus strand, and for each position, the percentage abundance of each nucleotide within the surrounding 100 nt is counted, with a sliding window of 1 nt. For clarity, only C (red line) and G (blue line) nucleotides are displayed. The C skew-containing region is indicated by the thick blue line at the bottom of the diagram. (*B*) The in vitro R loop formation assay indicates the participation of the *RPSAP52* transcript. The region containing the C skew (in blue) was cloned between the T7 and SP6 promoters, and in vitro transcription was carried out with either polymerase and in the presence of α-^{32}P-UTP. *HMGA2* transcription corresponds to T7 orientation, whereas antisense *RPSAP52* transcription is under the SP6 promoter (see diagram at left). To reveal RNA:DNA hybrids, the reactions were incubated in the absence (lanes 2 and 4) or presence (lanes 3 and 5) of bacterial recombinant RNaseH. After resolving in a 1% agarose gel, DNA bands were first stained with SYBRSafe (*Left*) and the same gel was then exposed for autoradiography to detect transcribed RNA (*Right*). As a control, a mock reaction without polymerase was also analyzed (lane 1). M, 1-kb DNA ladder. (*C*) MCF10A cells were transduced with lentiviral plasmids overexpressing control shRNA (scr) or shRNAs against *RPSAP52* RNA (sh1, sh4). RT-qPCR analysis of *HMGA2* and *RPSAP52* expression shows a clear reduction of both RNAs. Changes in expression for each case were calculated relative to control cells. Error bars show SDs calculated from two independent experiments. (*D*) Micrococcal nuclease accessibility assay on nuclei isolated from control (scr) or MCF10A cells overexpressing shRNAs against *RPSAP52* (sh1, sh4). The upper diagram indicates the fragments analyzed by qPCR along the *HMGA2* promoter. Regions R1–R6 are within the C skew. A–C fragments are control amplicons outside the C skew region. After chromatin digestion, levels of recovered DNA were estimated by qPCR with primer pairs for each indicated region. Each sample was first normalized against the Sat2 region (considered constant and highly compacted) to allow comparison between different nuclei preparations. For each primer pair, ΔCt values were calculated as Ct (0 min digestion) – Ct (10 min digestion), whereby higher values indicate more accessible chromatin. Final levels are presented relative to those of control transfected cells. Error bars, SDs from two independent experiments.

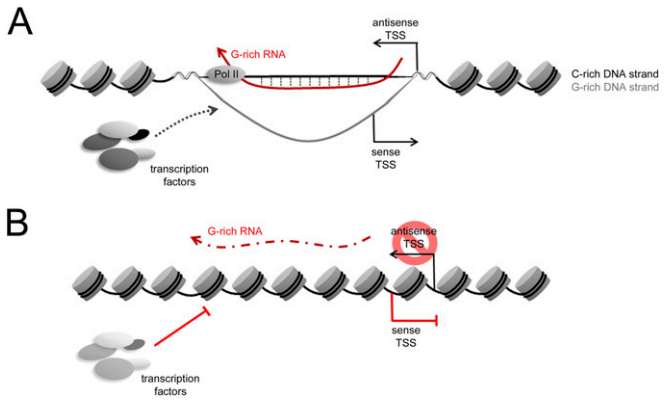

Fig. S8. A model for R loop involvement in transcriptional activation with the participation of antisense transcripts. (*A*) At the VIM locus (and possibly other sites of divergent transcription), an R loop is formed between the nascent, G-rich antisense transcript and the C-rich DNA strand. This structure maintains a local open chromatin conformation that allows for efficient recognition and binding of transcription factors, resulting in the sustained activation of nearby sense transcription. (*B*) Upon decrease of antisense transcription (for example, under hypermethylated conditions), R loop formation is prevented and the region remains compacted, inhibiting sense transcription.

Table S1. Primer sequences used in this work

Oligo name	Sequence 5′-3′
RNaseHdelMLSEcoRIfor	CTGGAATTCATGTTCTATGCCGTGAGGAGGG
RNaseHBamHIrev	CTGGGATCCCTAGTCTTCCGATTGTTTAGCTCC
shVIMAS2for	GATCCGGTGTACTAGTGAAGTGATTTCAAGAGAATCACTTCACTAGTACACCTTTTTTACGCGTG
shVIMAS2rev	AATTCACGCGTAAAAAAGGTGTACTAGTGAAGTGATTCTCTTGAAATCACTTCACTAGTACACCG
shVIMAS3for	GATCCGTCCAAATGTGCTACTCAGATTCAAGAGATCTGAGTAGCACATTTGGATTTTTTACGCGTG
shVIMAS3rev	AATTCACGCGTAAAAAATCCAAATGTGCTACTCAGATCTCTTGAATCTGAGTAGCACATTTGGACG
VIM_Afor	GCCTAAAAGAGGCTTGTCCA
VIM_Arev	CAGGGGGTACTGCAGGTTACT
VIM_Bfor	CGAAAACACCCTGCAATCTT
VIM_Brev	AATTGCTCGTGGGTTGTGTT
VIM_R1for	GGCCCAGCTGTAAGTTGGTA
VIM_R1rev	AGGGGAAACCGTTAGACCAG
VIM_R2for	GGACTGAGCCCGTTAGGTC
VIM_R2rev	CCTCTGTCCATCGACTTGC
VIM_R3for	CAATCTCAGGCGCTCTTTGT
VIM_R3rev	GAGCGGGAAGAGGAAAGAGT
VIM_R4for	ACCGGACCCCTCTGGTTC
VIM_R4rev	ACCCTGGGGTGCTGAAAA
VIM_R5for	GAAAGCCCCCAAAAGTCC
VIM_R5rev	CCTCGAGCCTTCCTGCTC
VIM_R6for	GAGGGGACCCTCTTTCCTAA
VIM_R6rev	GGAGCGAGAGTGGCAGAG
VIM_R7for	CCTCCTACCGCAGGATGTT
VIM_R7rev	GGTGGACGTAGTCACGTAGC
GAPDH_DRIPfor	AGAGAAACCCGGGAGGCTA
GAPDH_DRIPrev	TGACTCCGACCTTCACCTTC
qVIMfor	GGCTCAGATTCAGGAACAGC
qVIMrev	GCTTCAACGGCAAAGTTCTC
qVIM-AS1for	CAAAGCTCCCTTTGGATGAC
qVIM-AS1rev	ACTAGTACACCCCCGACGTG
VIMRloop1 for	TCTCCAAAGGCTGCAGAAGT
VIMRloop1rev	ATGATGTCCTCGGCCAGGTT
HMGA2Rloop1for	AGACGCTTCCTGCAAAGTGT
HMGA2Rloop1rev	TGGAGGTAGCAAGAGGAGGA
RLoop_st+_1_F1	AGACAGGCTTTAGCGAGTTATT
RLoop_st+_1_R1	AATAGGGATTTAGTGAGAAGTG
bsVIM_R1for	GATTTGAGGGATTTTTTATTTTTTT
bsVIM_R1rev	AAAAAATCCCCTCCCACT
bsVIM_R2for	GGGAGGGGATTTTTTTTTTA
bsVIM-R2rev	CAACTCCTACAACTCCACCTTC
HMGA2_Afor	GGGATGGAGGCTCTCTCTCT
HMGA2_Arev	CACTTTGCTGCACGTTGAGT
HMGA2_Bfor	TTGAGTAGGGGACGATCGAG
HMGA2_Brev	GCACGCTTAATTGGTTGCAT
HMGA2_Cfor	ATTTAGACTGGAGGCCATGC
HMGA2_Crev	TGGGAGGTTTTGCTTGAATC
HMGA2_1for	CTCCGGGACAGTCACGTT
HMGA2_1rev	CTAGCTCCACCCGCCTCT
HMGA2_3for	CACGATTAGAGGTGGGCACT
HMGA2_3rev	TGTGAGTGTGAGTGTGTGTGG
HMGA2_4for	GAATCTTGGGGCAGGAACTC
HMGA2_4rev	GGCTGCTAGCTCCTGAGTCTT
HMGA2_5for	GGTGCCACCCACTACTCTGT
HMGA2_5rev	CAAAGGAGGATGGGGAGACT
HMGA2_6for	GCAACTCCTGATCCCAACC
HMGA2_6rev	TGGAGGTAGCAAGAGGAGGA